Metrol. Meas. Syst., Vol. 24 (2017), No. 2, pp. 337–346.

PAN POLSKA AKADEMIA NAUK

METROLOGY AND MEASUREMENT SYSTEMS

Index 330930, ISSN 0860-8229

www.metrology.pg.gda.pl

M&MS

RAPID DESIGN OPTIMIZATION OF MULTI-BAND ANTENNAS BY MEANS OF RESPONSE FEATURES

Sławomir Kozieł, Adrian Bekasiewicz

Reykjavik University, School of Science and Engineering, Menntavegur 1, 101 Reykjavik, Iceland
(koziel@ru.is, ✉ bekasiewicz@ru.is, +354 599 6886)

Abstract

This work examines the reduced-cost design optimization of dual- and multi-band antennas. The primary challenge is independent yet simultaneous control of the antenna responses at two or more frequency bands. In order to handle this task, a feature-based optimization approach is adopted where the design objectives are formulated on the basis of the coordinates of so-called characteristic points (or response features) of the antenna response. Due to only slightly nonlinear dependence of the feature points on antenna geometry parameters, optimization can be attained at a low computational cost. Our approach is demonstrated using two antenna structures with the optimum designs obtained in just a few dozen of EM simulations of the respective structure.

Keywords: antenna design, antenna measurements, computer-aided design, surrogate modelling, feature-based optimization.

1. Introduction

Contemporary antenna engineering heavily relies on full-wave *electromagnetic* (EM) analysis. EM solvers offer accurate performance analysis, as well as account for interactions of the structure with environmental components (*e.g.* connectors, housing) [1, 2]. However, EM simulations tend to be expensive, especially for complex structures, so that their use in automated design, *e.g.* parametric optimization, may be impractical [3]. EM-driven design becomes even more challenging in the case of multi-objective design (*e.g.* antenna size vs. electrical performance) [4, 5] or in the case of dual- and multi-band antennas, where requirements on the reflection response have to be satisfied for several frequency bands of interest [6, 7]. Traditional methods involving parameter sweeps become problematic in such cases, especially for compact antennas with considerable EM cross-couplings, that make independent control of frequency bands difficult [8].

Computationally efficient EM-driven design of antennas can be achieved by means of *surrogate-based optimization* (SBO) methods [9, 10]. SBO involving physics-based surrogates are particularly promising due to combining the speed of the underlying low-fidelity model and reasonable accuracy obtained by applying suitable correction techniques. The low-fidelity models are typically obtained from coarse-discretization EM simulations. The popular methods for surrogate construction include space mapping [10], frequency scaling [10], shape-preserving response prediction [11], adaptive response correction [12], manifold mapping [13], and adaptively adjusted design specifications [14]. Combining physics-based modelling with data-driven modelling may also produce promising results [1, 5]. In terms of conventional optimization methods, only gradient-based search seems to ensure comparable efficiency if derivative data are obtained through cheap adjoint sensitivities [15, 16].

Recently, *feature-based optimization* (FBO) has been proposed for the design of microwave filters [17], where the original design problem is reformulated in a so-called feature space,

Article history: received on Oct. 14, 2016; accepted on Jan. 21, 2017; available online on Jun. 30, 2017; DOI: 10.1515/mms-2017-0030.

leading to a less nonlinear functional landscape to be optimized compared with the original formulation (typically, w.r.t. *S*-parameters versus frequency). This work is based on our original conference publication of [18], where FBO concept has been adopted for the design of dual-band antennas. Here, we reformulate the considered framework to allow for optimization of multi-band structures.". We demonstrate that reformulating the antenna design task with the use of suitably defined features leads to considerable simplifications, so that the optimization process can be accomplished at a much lower computational cost compared with that of conventional algorithms. Two application examples are provided. Numerical results are supported by experimental verification of the fabricated antenna prototypes.

2. Feature-based optimization for multi-band antennas

The purpose of this section is to formulate a feature-based optimization algorithm for multi-band antenna design. There are several challenges that need to be addressed, such as highly nonlinear responses, multiple objectives (in particular, independent control of several operating frequencies), but also a large number of adjustable geometry parameters of the antenna at hand.

2.1. Response features of dual-band antennas

Figure 1 shows typical responses of a dual-band antenna and, more importantly, their changes resulting from modification of the antenna geometry (the responses correspond to the example considered in Section 3.1). The responses are evaluated along a selected line segment in the design space defined as $\boldsymbol{y}(t) = t\cdot\boldsymbol{y}^1 + (1 - t)\cdot\boldsymbol{y}^2$, where $0 \le t \le 1$, whereas $\boldsymbol{y}^1$ and $\boldsymbol{y}^2$ are the two reference designs. High nonlinearity and considerable variability of the responses can be observed. Fig. 2 shows changes of the response features, here selected as the minima of the reflection responses (*i.e.* the points corresponding to the antenna resonances) and the point corresponding to –10 dB reflection levels. Each point is described by its two coordinates (frequency and level). Note that, despite of a high nonlinearity of the reflection response, the behavior of the feature points is close to linear. Consequently, expressing the design goals based on the feature points and using feature-based surrogates, the optimization process is expected to be considerably speeded up .

2.2. Antenna design in feature space

The original design problem (in *S*-parameter vs. frequency domain) is formulated as:

$$\boldsymbol{x}^* = \arg\min_{x} U(\boldsymbol{R}(\boldsymbol{x})), \tag{1}$$

where U is an objective function defined with the EM model response, *i.e.* S_{11} versus frequency.

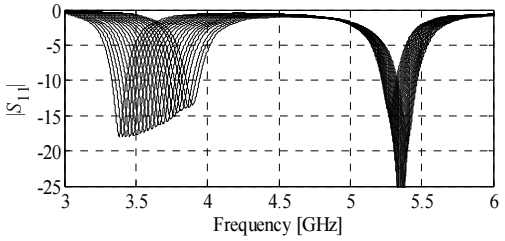

Fig. 1. A family of dual-band responses corresponding to their geometries along a certain line segment in the design space showing highly nonlinear dependence of the reflection characteristic on the geometry variables of the structure.

Given several operating frequencies f_k, $k = 1, \ldots, N_f$, for a multi-band antenna, a typical formulation would be to minimize max $\{|S_{11}(\boldsymbol{x})|$ at $f_1, \ldots, |S_{11}(\boldsymbol{x})|$ at $f_{Nf}\}$ in respect to $\boldsymbol{x}$ (in particular to ensure that the reflection is less than –10 dB at all frequencies). Another option could be to maximize the antenna bandwidth around the operating frequencies. In any case, in (1) one needs to directly handle highly nonlinear responses, as shown in Fig. 1.

Here, the design task is reformulated based on the feature vectors $\boldsymbol{F}(\boldsymbol{x})$ and $\boldsymbol{L}(\boldsymbol{x})$ (*i.e.* frequency and level coordinates of the respective feature points), as follows:

$$\boldsymbol{x}^* = \arg\min_{\boldsymbol{x}} U_F(\boldsymbol{F}(\boldsymbol{x}), \boldsymbol{L}(\boldsymbol{x})), \tag{2}$$

where U_F is an appropriate objective function. The major advantage of this formulation is that the functional landscape of the problem (2) is much less nonlinear than that for the original problem (1). Also, because of handling the frequencies of the feature points, it is possible to easily control the frequency location of the resonances, which is difficult in (1).

If the goal is to minimize antenna reflection at the operating frequencies f_k, the function U_F uses only N_f feature points $[f^{(1)}(\boldsymbol{x})\ l^{(1)}(\boldsymbol{x})]$, …, $[f^{(Nf)}(\boldsymbol{x})\ l^{(Nf)}(\boldsymbol{x})]$ corresponding to the reflection response minima, and is defined as follows:

$$U_F(\boldsymbol{x}) = \max\{l^{(1)}(\boldsymbol{x}),\ldots,l^{(N_f)}(\boldsymbol{x})\} + \beta\left\|\begin{bmatrix} f^{(1)}(\boldsymbol{x}) \\ \vdots \\ f^{(N_f)}(\boldsymbol{x}) \end{bmatrix} - \begin{bmatrix} f_1 \\ \vdots \\ f_{Nf} \end{bmatrix}\right\|^2. \tag{3}$$

It can be observed that, according to (3), the main objective is to minimize antenna reflection. On the other hand, the penalty term enables to control the operating frequencies of the structure. It should be noted that the values of the coefficient β should be sufficiently large to ensure that the contribution of the penalty term is comparable to the primary objective for an unacceptably large frequency allocation error (we use $\beta = 100$).

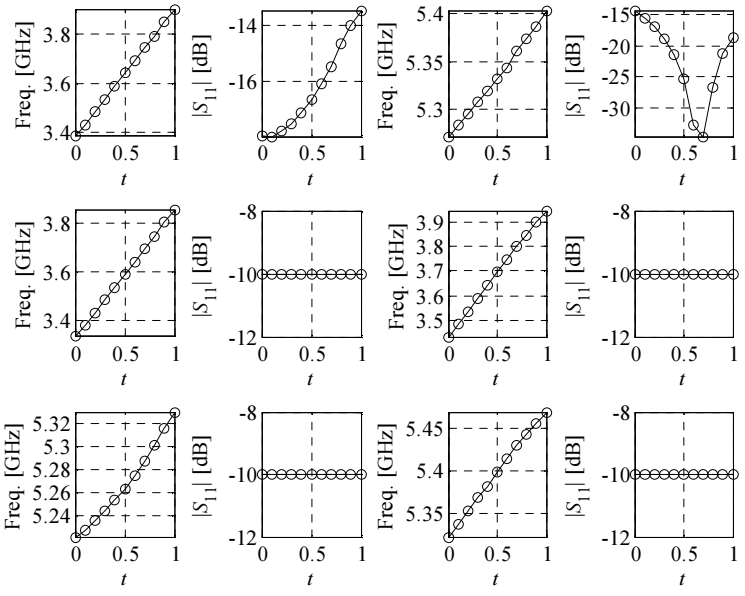

Fig. 2. The feature points (the reflection minima and the points corresponding to –10 dB levels), as described in Section II.*1*, corresponding to antenna geometries along the same line segment parameterized by *t* as in Fig. 1.

2.3. Optimization algorithm

The problem (2) is solved iteratively as:

$$\boldsymbol{x}^{(i+1)} = \arg\min_{\|\boldsymbol{x}-\boldsymbol{x}^{(i)}\|\le r^{(i)}} U_F(\boldsymbol{F}_S^{(i)}(\boldsymbol{x}), \boldsymbol{L}_S^{(i)}(\boldsymbol{x})), \tag{4}$$

where $\boldsymbol{x}^{(i)}$, i = 0, 1, …, is a sequence approximating $\boldsymbol{x}^*$, whereas $\boldsymbol{F}_S^{(i)}$ and $\boldsymbol{L}_S^{(i)}$ are linear approximation models of the feature point vectors $\boldsymbol{F}(\boldsymbol{x})$ and $\boldsymbol{L}(\boldsymbol{x})$ determined in the current design $\boldsymbol{x}^{(i)}$. Finite differentiation is used to establish the models with n perturbed designs around $\boldsymbol{x}^{(i)}$, *i.e.*, $\boldsymbol{x}^{(i)} + \boldsymbol{h}_k$, k = 1, …, n, where $\boldsymbol{h}_k = [0 \ldots 0\ d_k\ 0 \ldots 0]^T$, $d_k > 0$ [19], and the corresponding feature points $\boldsymbol{F}(\boldsymbol{x}^{(i)} + \boldsymbol{h}_k)$, $\boldsymbol{L}(\boldsymbol{x}^{(i)} + \boldsymbol{h}_k)$ are extracted from the respective antenna responses. We have:

$$\boldsymbol{F}_S^{(i)}(\boldsymbol{x}) = \boldsymbol{F}(\boldsymbol{x}^{(i)}) + \begin{bmatrix} [\boldsymbol{F}(\boldsymbol{x}^{(i)} + \boldsymbol{h}_1) - \boldsymbol{F}(\boldsymbol{x}^{(i)})]^T / d_1 \\ \ldots \\ [\boldsymbol{F}(\boldsymbol{x}^{(i)} + \boldsymbol{h}_n) - \boldsymbol{F}(\boldsymbol{x}^{(i)})]^T / d_n \end{bmatrix}^T \cdot (\boldsymbol{x} - \boldsymbol{x}^{(i)}), \tag{5}$$

$$\boldsymbol{L}_S^{(i)}(\boldsymbol{x}) = \boldsymbol{L}(\boldsymbol{x}^{(i)}) + \begin{bmatrix} [\boldsymbol{L}(\boldsymbol{x}^{(i)} + \boldsymbol{h}_1) - \boldsymbol{L}(\boldsymbol{x}^{(i)})]^T / d_1 \\ \ldots \\ [\boldsymbol{L}(\boldsymbol{x}^{(i)} + \boldsymbol{h}_n) - \boldsymbol{L}(\boldsymbol{x}^{(i)})]^T / d_n \end{bmatrix}^T \cdot (\boldsymbol{x} - \boldsymbol{x}^{(i)}). \tag{6}$$

The algorithm (4) is embedded in a trust-region framework with the search radius $r^{(i)}$ updated using standard rules [19].

3. Verification examples

In this section, the considered feature-based method for fast design of multi-band antennas is verified. Two design examples are considered: a dual-band patch antenna with 8 design variables and a triple-band uniplanar dipole with 10 adjustable parameters. For the latter structure, the numerical results are supported with measurements of the fabricated antenna prototypes.

3.1. Dual-band patch antenna

Our first example is concerned with verification of a dual-band planar antenna shown in Fig. 3 [20]. The structure consists of two radiating elements in the form of a quasi-micro-strip patch with an inset feed and a monopole radiator, both connected in a cascade. The antenna is excited through a 50 ohm microstrip line. The lower and upper resonant frequencies are introduced by the monopole and the patch, respectively. The ground plane is trimmed below the patch component to increase the number of degrees of freedom (hence, it is referred to as a quasi-micro-strip patch).

The antenna is constructed on a 0.762 mm thick Taconic RF-35 dielectric substrate with a relative permittivity of 3.5 and a loss tangent of 0.0018. The design variables are $\boldsymbol{x} = [L\ l_1\ l_2\ l_3\ W\ w_1\ w_2\ g]^T$. The parameters o = 7, w_0 = 1.7, l_0 = 10, and s = 0.5 are fixed. The unit for all parameters is mm. The lower and upper bounds for the parameters are $\boldsymbol{l} = [10\ 1\ 5\ 1\ 4\ 0.2\ 1\ {-4}]^T$ and $\boldsymbol{u} = [20\ 6\ 17\ 7\ 16\ 4\ 6\ 6]^T$, respectively. Note that negative g results in trimming ground plane below the patch component of the radiator

The EM antenna model $\boldsymbol{R}$ is implemented in CST Microwave Studio and contains ~1,900,000 hexahedral mesh cells. Its average simulation time on a dual Xeon E5540 machine with 6 GB RAM is 12 minutes.

Two cases were considered regarding the design requirements:

- Case I: operating frequencies 3.5 GHz and 5.3 GHz;
- Case II: operating frequencies 2.4 GHz and 4.8 GHz.

In both cases, the goal is to allocate the resonances at the respective operating frequencies and to minimize reflection at these frequencies. The initial design is $\boldsymbol{x}^{\text{init}}$ = [17.0 1.8 11.7 4.1 12.9 0.7 1.3 0.2]^T mm. As shown in Fig. 4, this design is poor and very far from satisfying design specifications in both considered cases. More importantly, as the reflection response is flat and close to zero in the initial design in the vicinity of the operating frequencies, local optimization would be stuck in the initial design when the original formulation of the problem is considered (cf. (1)). This was verified using a pattern-search algorithm [21]. Consequently, global optimization methods would have to be used with an associated very high computational cost.

Figure 4 shows the antenna responses in the initial and in the final design $\boldsymbol{x}^{*\text{I}}$ = [17.17 2.19 13.20 5.00 12.78 0.94 4.00 2.62]^T mm found by FBO. Note that the design quality is very good with the resonances well centred at the operating frequencies of interest and with the reflection levels < -25 dB.

The optimization cost was 72 evaluations of the EM model (8 algorithm iterations), which is low, given the complexity of the problem and the fact that FBO is a derivative-free method. Local optimization working for the original formulation of the problem failed to find an acceptable design.

Figure 5 shows the results for Case II. The optimum design is $\boldsymbol{x}^{*\text{II}}$ = [17.64 2.89 13.84 6.90 13.55 0.20 5.03 4.09]^T mm, and it was obtained at the cost of 90 evaluations of the EM antenna model (10 algorithm iterations). Again, the design quality is very good with resonances centred at the operating frequencies and the reflection minima below –30 dB. Note that the optimum design is at a considerable distance from the initial one (response-wise). If the optimization starts from $\boldsymbol{x}^{*\text{I}}$, a solution comparable to $\boldsymbol{x}^{*\text{II}}$ is obtained in just four iterations.

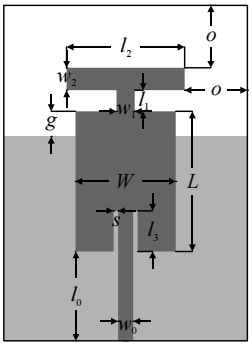

Fig. 3. The dual-band patch antenna geometry [20]. The ground plane is marked using the lighter shade of grey.

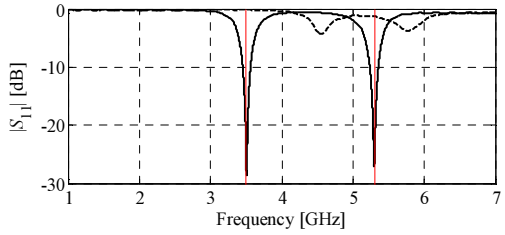

Fig. 4. The optimization results, Case I. Antenna responses in the initial design (- - -) and in the design found by the feature-based optimization algorithm (—).

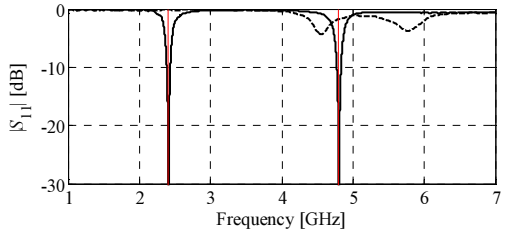

Fig. 5. The optimization results, Case II. Antenna responses in the initial design (- - -) and in the design found by the feature-based optimization algorithm (—).

3.2. Triple-band planar dipole antenna

Our second example is a triple-band uniplanar dipole antenna shown in Fig. 6. The structure is based on the geometry introduced in [22]. The used substrate is a 0.762 mm thick Taconic RF-35 (see Section 3.1). The antenna is constructed as a stack of three narrow, long ground plane slits separated by two thicker, short slots. The radiator is fed through a 50 ohm coplanar waveguide (CPW). The vector of adjustable parameters is $\boldsymbol{x} = [l_1\ l_2\ l_3\ l_4\ l_5\ w_1\ w_2\ w_3\ w_4\ w_5]^T$, whereas dimensions $l_0 = 30$, $w_0 = 3$, $s_0 = 0.15$ and $o = 5$ remain fixed. The unit for all geometric parameters is mm. The search space is defined using the following lower and upper bounds: $\boldsymbol{l} = [30\ 5\ 22\ 5\ 15\ 0.2\ 1.2\ 0.2\ 1.2\ 0.2]^T$ and $\boldsymbol{u} = [50\ 15\ 29\ 15\ 21\ 2.2\ 4.2\ 2.2\ 4.2\ 2.2]^T$. The EM antenna model $\boldsymbol{R}$ (~100,000 cells; simulation: 6 min) is prepared in CST Microwave Studio and simulated using its time domain solver.

Two sets of design specifications are considered:

- Case I: operating frequencies: 2.45 GHz, 3.65 GHz, and 5.77 GHz;
- Case II: operating frequencies: 1.85 GHz, 2.95 GHz, and 5.15 GHz.

Similarly to Section 3.1, the goal of the optimization was to minimize the antenna reflection for the selected operating frequencies. The initial design parameters are $\boldsymbol{x}^{\text{init}} = [36\ 14\ 26\ 12\ 20\ 1\ 3\ 1\ 2\ 1]^T$ mm. As it can be seen from Fig. 7, the initial design is closer to the desired specifications compared with the example discussed in Section 3.1. Consequently, for the Case I, the original formulation of the design problem given by (1) can be used to find the desired design solution using a local search algorithm (here, the pattern-search one). However, for the Case II, the algorithm was stuck at the local minimum which was away from the desired solution.

For Case I, the comparison of the antenna responses in the initial design and in the design optimized using the feature-based method is shown in Fig. 7. The final vector of parameters is $\boldsymbol{x}^{*\text{I}} = [39.04\ 14.99\ 28.26\ 12.26\ 18.91\ 1.20\ 1.2\ 0.2\ 1.35\ 0.77]^T$. It should be noted that the structure response is well centred at the chosen operating frequencies with the reflection levels below –22 dB.

The cost of the algorithm operation was 130 evaluations of the antenna model (12 iterations). At the same time, the pattern-search algorithm required 278 EM simulations to obtain a similar antenna solution. Thus, for the considered case, the numerical cost of pattern-search optimization is almost 50 percent higher than that of FBO.

For Case II, the vector of optimal parameters is: $\boldsymbol{x}^{*\text{II}} = [45.28\ 9.48\ 28.99\ 10.63\ 19.29\ 1.45\ 3.55\ 0.62\ 1.68\ 0.43]^T$. The frequency characteristics of the structure in the initial and optimized design are compared in Fig. 8. Again, the antenna features good electrical performance at the selected operating frequencies with the reflection level below –12 dB.

The numerical cost of the design process is 100 evaluations of the EM antenna model (9 iterations). Having in mind noticeable distance of the first two operating frequencies from the initial design, the cost is very low.

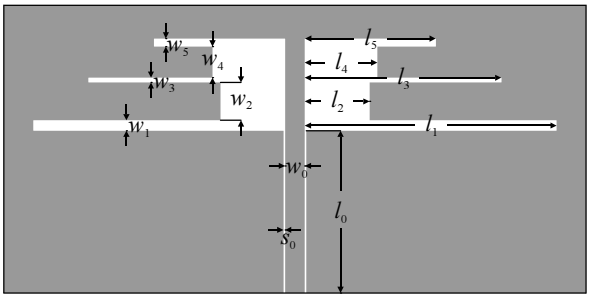

Fig. 6. The triple-band dipole antenna geometry with highlighted design parameters.

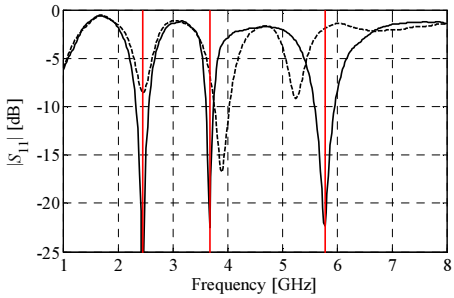

Fig. 7. The triple-band dipole antenna optimization results: Case I. Antenna responses in the initial design (- - -) and in the design found by the feature-based optimization algorithm (—).

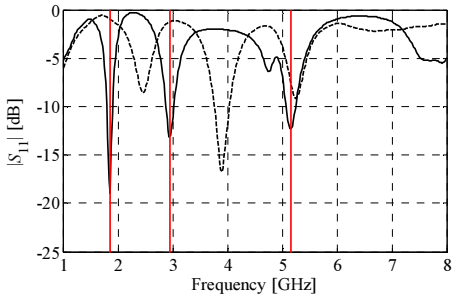

Fig. 8. The triple-band dipole antenna optimization results: Case II. Antenna responses in the initial design (- - -) and in the design found by the feature-based optimization algorithm (—).

The results obtained for both antenna designs have been experimentally validated. Photographs of the fabricated structures are shown in Fig. 9, whereas Fig. 10 presents comparison of their simulated and measured reflection characteristics. For Case I, the measured lowest operating frequency is slightly shifted down by about 50 MHz. Nonetheless, the remaining bands are well aligned. For Case II (Fig. 10(b)), the measured bandwidth is slightly broader around the second operating frequency compared with the simulated one. The difference, however, is only about 60 MHz. Generally, the results are in a good agreement. Small discrepancies between the simulated and measured responses are due to the use of a simplified antenna EM model without an EM connector. The latter has been excluded from simulations in order to reduce the computational cost of the optimization process.

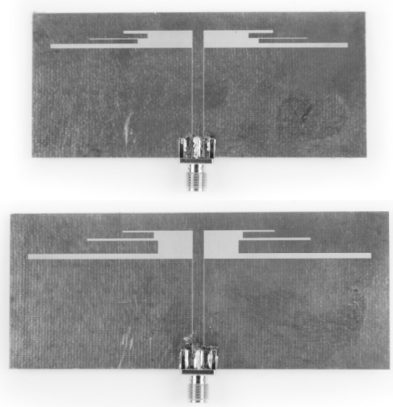

Fig. 9. Photographs of the fabricated dipole antenna prototypes: Case I (top), and Case II (bottom).

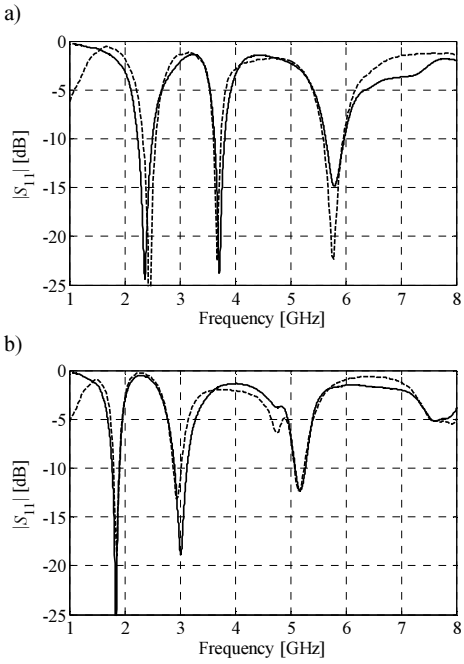

Fig. 10. Comparison of the simulated (– –) and measured (—) reflection characteristics obtained for the triple-band dipole antenna: Case I (a); and Case II (b).

4. Conclusion

Rapid and precise design optimization of dual- and multi-band antennas has been presented. The key component of the optimization procedure that ensures its computational efficiency is reformulation of the design problem in a feature space of suitably-defined characteristic points, where the objectives are less nonlinear functions of the geometry parameters of the antenna (as compared with the original formulation, typically, in the space of *S*-parameters versus frequency). This enables to yield the optimized design at a low cost corresponding to just a few dozen of EM simulations. Working examples of a dual- and triple-band antennas as well as their experimental verification confirm validity of the proposed approach. Our further work will

focus on application to the method for other multi-band microwave structures, such as filters, couplers or power dividers.

Acknowledgement

The authors would like to thank Computer Simulation Technology AG, Darmstadt, Germany, for making CST Microwave Studio available. This work is partially supported by the Icelandic Centre for Research (RANNIS) Grants 141272051, 163299051 and by National Science Centre of Poland Grant 2014/15/B/ST7/04683.

References

[1] Bekasiewicz, A., Koziel, S. (2015). Structure and computationally-efficient simulation-driven design of compact UWB monopole antenna. *IEEE Ant. Wireless Prop. Lett.*, 14, 1282–1285.

[2] Koziel, S., Ogurtsow, S., Zieniutycz, W., Bekasiewicz, A. (2015). Design of a planar UWB dipole antenna with an integrated balun using surrogate-based optimization. *IEEE Ant. Wireless Prop. Lett.*, 14, 366–369.

[3] Lizzi, L., Viani, F., Azaro, R., Massa, A. (2007). Optimization of a spline-shaped UWB antenna by PSO. *IEEE Ant. Wireless Prop. Lett.*, 6, 182–185.

[4] Chamaani, S., Abrishamian, M.S., Mirtaheri, S.A. (2010). Time-domain design of UWB Vivaldi antenna array using multiobjective particle swarm optimization. *IEEE Ant. Wireless Prop. Lett.*, 9, 666–669.

[5] Koziel, S., Bekasiewicz, A. (2015). Fast multi-objective optimization of narrow-band antennas using RSA models and design space reduction. *IEEE Ant. Wireless Prop. Lett.*, 14, 450–453.

[6] Bod, M., Hassani, H.R., Taheri, M.M.S. (2012). Compact UWB printed slot antenna with extra Bluetooth, GSM, and GPS bands. *IEEE Ant. Wireless Prop. Lett.*, 11, 531–534.

[7] Liu, Y.F., Wang, P., Qin, H. (2014). Compact ACS-fed UWB monopole antenna with extra Bluetooth band. *Electronics Lett.*, 50(18), 1263–1264.

[8] Wang, L., Xu, L., Chen, X., Yang, R., Han, L., Zhang, W. (2014). A compact ultrawideband diversity antenna with high isolation. *IEEE Ant. Wireless Prop. Lett.*, 13, 35–38.

[9] Queipo, N.V., Haftka, R.T., Shyy, W., Goel, T., Vaidynathan, R., Tucker, P.K. (2005). Surrogate-based analysis and optimization. *Prog. Aerospace Sci.*, 41(1), 1–28.

[10] Bandler, J.W., Cheng, Q.S., Dakroury, S.A., Mohamed, A.S., Bakr, M.H., Madsen, K., Søndergaard, J. (2004). Space mapping: the state of the art. *IEEE Trans. Microwave Theory Tech.*, 52(1), 337–361.

[11] Koziel, S., Ogurtsov, S., Szczepanski, S. (2012). Rapid antenna design optimization using shape-preserving response prediction. *Bulletin of the Polish Academy of Sciences. Tech. Sci.*, 60, 143–149.

[12] Koziel, S., Bandler, J.W., Madsen, K. (2005). Towards a rigorous formulation of the space mapping technique for engineering design. *IEEE Int. Symp. Circuits Syst.*, 6, 5605–5608.

[13] Koziel, S., Leifsson, L., Ogurtsov, S. (2013). Reliable EM-driven microwave design optimization using manifold mapping and adjoint sensitivity. *Microwave Opt. Tech. Lett.*, 55, 809–813.

[14] Koziel, S., Ogurtsov, S. (2013). Rapid optimization of omnidirectional antennas using adaptively adjusted design specifications and kriging surrogates. *IET Microwaves, Ant. Prop.*, 7(15), 1194–1200.

[15] El Sabbagh, M.A., Bakr, M.H., Bandler, J.W. (2006). Adjoint higher order sensitivities for fast full-wave optimization of microwave filters. *IEEE Trans. Microw Theory Tech.*, 54, 3339–3351.

[16] Koziel, S., Bekasiewicz, A. (2015). Fast EM-driven size reduction of antenna structures by means of adjoint sensitivities and trust regions. *IEEE Ant. Wireless Prop. Lett.*, 14, 1681–1684

[17] Koziel, S., Bandler, J.W. (2015). Rapid yield estimation and optimization of microwave structures exploiting feature-based statistical analysis. *IEEE Trans. Microwave Theory Tech.*, 63(1), 107–114.

[18] Koziel, S., Bekasiewicz, A., Leifsson, L. (2016). Expedited design of dual-band antennas using feature-based optimization. *European Conf. Ant. Prop.*, Davos, 1–4.

[19] Conn, A.R., Gould, N.I.M., Toint, P.L. (2000). *Trust-region methods*. MPS-SIAM Series on Optimization, Philadelphia.

[20] Koziel, S., Bekasiewicz, A., Leifsson, L. (2016). Rapid EM-driven antenna dimension scaling through inverse modeling. *IEEE Ant. Wireless Prop. Lett.*, 15, 714–717.

[21] Kolda, T.G., Lewis, R.M., Torczon, V. (2003). Optimization by direct search: new perspectives on some classical and modern methods. *SIAM Review*, 45(3), 385–482.

[22] Chen, Y.C., Chen, S.Y., Hsu, P. (2006). Dual-band slot dipole antenna fed by a coplanar waveguide. *IEEE Int. Symp. Ant. Prop.*, 3589–3592.